Dry layer preparation and characterisation of polymer electrolyte fuel cell components

E. Gülzow [*], M. Schulze, N. Wagner, T. Kaz, R. Reissner, G. Steinhilber, A. Schneider

Deutsches Zentrum für Luft- und Raumfahrt (DLR), Institut für Technische Thermodynamik, Pfaffenwaldring 38-40, D-70569 Stuttgart, Germany

Abstract

The main problem for future fuel cell commercialisation is the cost of membrane–electrode assemblies (MEAs) satisfying both power density and lifetime requirements. At DLR, low-cost MEA production techniques are being developed. These new MEAs are characterised and investigated with physical and electrochemical methods in order to study the power loss processes, the lifetime, the reaction mechanisms and in support of MEA development. The possibilities for the characterisation methods used will be demonstrated by various examples. At DLR, a new production technique based on the adaptation of a rolling process is developed for fuel cell electrode and MEA preparation. After mixing the dry powder electrode material in a mill, it is blown onto the membrane (or backing) resulting in a uniformly distributed layer. This reactive layer is fixed and thoroughly connected to the membrane by passing them through a calender. In order to produce the second electrode, the same steps are repeated. This procedure is very simple and, as a dry process, avoids the use of any solvents and drying steps. We have achieved a thickness of the reactive layer as low as 5 μm, reducing the amount of catalyst needed and, thus, the costs. Electrochemical investigations have shown a performance comparable to that of commercial electrodes. The degradation of MEA for polymer membrane fuel cell (PEFC) components during the cell's lifetime, yields a change in the electrochemical behaviour. The characterisation of PEFC MEA-components after electrochemical operation has given information about the degradation of electrodes and membranes and about the change in the platinum distribution on the anode, whilst on the cathode, the platinum content is unchanged. © 2000 Elsevier Science S.A. All rights reserved.

Keywords: Membrane–electrode assemblies; Polymer membrane fuel cell; Dry layer preparation

1. Introduction

Much attention has been paid to fuel cells because they offer a highly efficient and environmentally benign technology for energy conversion avoiding the Carnot limitations of combustion engines, which are constrained to produce work at a much higher flame temperature. Polymer membrane fuel cells (PEFCs) and direct methanol fuel cells (DMFCs) are considered as most promising options for powering future cars [1] and small combined power units due to their modular construction and the high energy densities that can be attained.

An important research and development goal is to produce efficient, cheap electrodes and membrane–electrode assemblies (MEAs). There is especially a need for production technologies of electrodes and MEAs that allow mass production of reproducible electrodes [2,3]. Usually, elec-

trodes are prepared from a suspension of the supported carbon black catalyst, PTFE and electrolyte. The suspension is applied to a carrier and then dried [4–7]. The possibility of transferring this procedure to an industrial, cheap mass production technique is questionable.

In order to systematically improve the efficiency of the fuel cell, a better understanding of the reactions and mass transport in the cell is essential. Moreover, quality control and understanding of degradation need a detailed characterisation and a better comprehension of experimental results [8].

The characterisation of the electrodes was performed by electrochemical analysis as well as physical methods on both single electrodes and MEAs. In addition to V–I characteristics, the electrodes were electrochemically measured by cyclic voltammetry (CV), electrochemical impedance spectroscopy (EIS) and chronopotentiometry [9–21]. To determine the pore structures, nitrogen adsorption and mercury porosimetry were used. Chemical composition and microstructure of the electrodes were studied

* Corresponding author. Fax: +49-711-6862-747; e-mail: erich.guelzow@dlr.de

by surface science methods, such as scanning electron microscopy (SEM), energy disperse X-ray spectroscopy (EDX), X-ray induced photoelectron spectroscopy (XPS) and porosimetry with nitrogen adsorption and Hg-porosimetry [18–25].

Commercial electrodes and MEAs were characterised in the same way as DLR dry-produced electrodes and their results were compared.

2. Preparation technique

The aim of the preparation process development at DLR was to achieve a low-cost and effective manufacturing process for PEFC MEAs. Therefore, a novel technique for MEA production was developed at DLR [26a,26b]. This process is based on other dry production techniques developed at DLR [2,3,20,27–29]. The fundamental idea for this simple process is to spray a dry catalytic layer directly onto the membrane to avoid waiting times for evaporating solvents and at the same time, to accomplish good contact between the catalytic layer and the electrolyte membrane. Therefore, it was necessary to develop a dry coating system that can handle fine powders (< 0.1 μm diameter) like carbon-supported catalysts (e.g., Pt on Vulcan XC-72).

The preparation process for MEAs is divided into three main steps:
1. Preparation of the electrode powder
2. Dry spraying the powder onto the membrane
3. Hot rolling or pressing the membrane with the gas diffusion layers

Fig. 1 shows a scheme of the manufacturing process. The first main preparation step for MEA production comprises mixing of the reactive layer material (e.g., platinum supported on carbon black with different amounts of PTFE, polymer electrolyte powder and/or filler materials) in a

knife mill [2,30]. In order to obtain homogeneous and thin reactive layers, the material is atomised and sprayed in a nitrogen stream through a slit nozzle directly on a membrane. The adhesion of the catalytic layer material onto the surface is already secure. However, in order to improve the electrical and ionic contact, it is necessary to fix the layer by hot rolling or pressing. Depending on the degree atomisation of a completely uniformly covered reactive layer, with thickness down to 5 μm, can be prepared using the production technique described. This fact yields to a low noble metal catalyst loading.

In addition to the preparation of the reaction layers, this technique can also be used to form a hydrophobic coverage for the surface of the MEA backing material, especially as this preparation step of the electrode production is also free of solvents.

From the low catalyst loading combined with the simplicity and degree of automation of the procedure, it is clear that the aim of a low-cost production technique can be achieved. By changing the composition of the raw powder and the deposition conditions of subsequent layers, it is possible to establish gradients, for instance, in porosity, catalyst loading or hydrophobicity in electrodes for other applications, for example, for DMFC. Another advantage of this production technique is that environmentally hazardous solvents are totally avoided. In addition, this technique can be scaled up to an industrial production process. From all the advantages, it is clear that our procedure has the capability to become an important industrial production technique for fuel cell MEA.

The electrode raw powder for standard MEAs consists of 20 wt.% PTFE (Hostaflon TF 2053 from Hoechst) and 80 wt.% carbon-supported Pt (20 wt.% Pt on Vulcan XC-72 from E-TEK) and is mixed in a knife mill for 5 s. In the next step, the powder is transferred to a sprayer where it is sprayed on the membrane in thin layers by
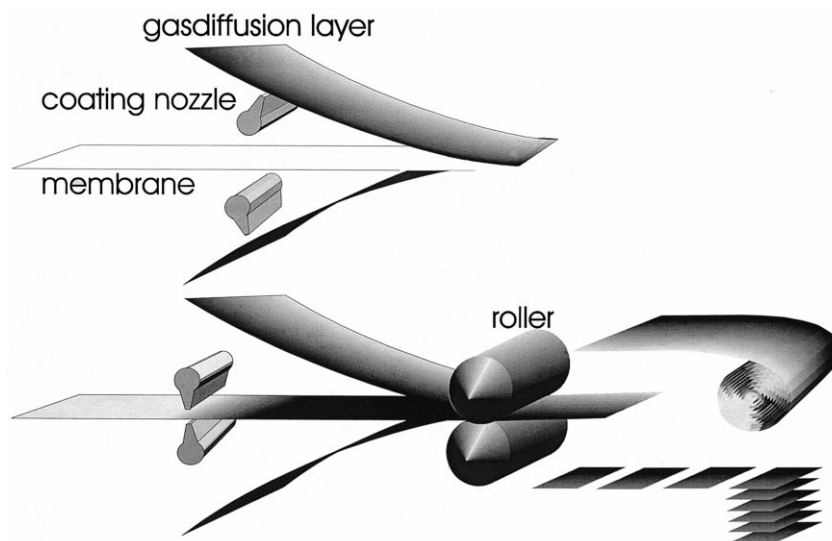

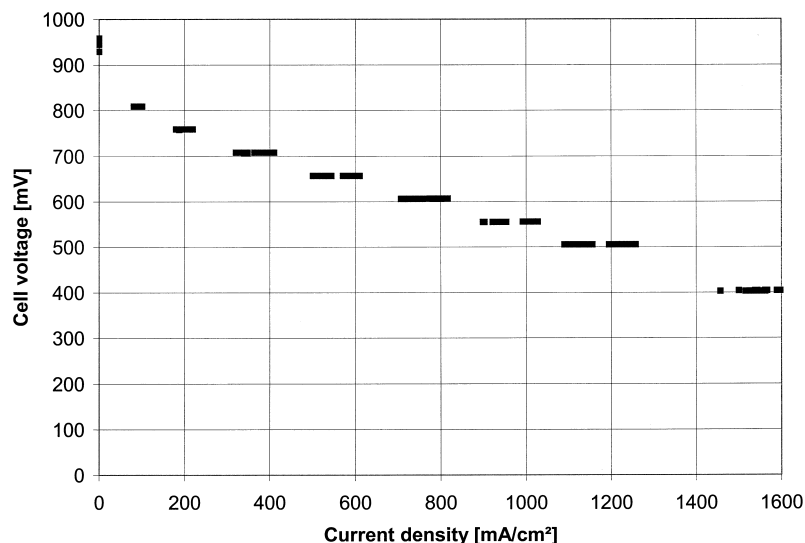Fig. 1. Scheme of the dry production technique for PEFC and DMFC MEAs.

Fig. 2. *V–I* characteristics of an MEA structure with Nafion 112 membrane; Pt-loading 0.07 mg/cm^2, 80°C, $p_{H_2} = p_{O_2} = 2$ bar.

moving the membrane over a coating nozzle. Thereby, various Pt-loadings up to 4 mg/cm^2 and down to 0.05 mg/cm^2 are possible. To fix the catalytic layer and to complete the MEA, gas-diffusion layers are hot-rolled or -pressed onto the coated membrane. Fig. 2 shows the performance of a standard MEA with Nafion 112 membrane and a Pt-loading of 0.07 mg/cm^2 on each electrode.

3. Electrochemical characterisation

The electrochemical characterisation of the electrodes was performed in a single fuel cell with a geometric area

of 23 cm^2. The fuel cell test setup is completely automated and controlled by a computer and SPS. With this device, it is possible to adjust and control the operating conditions, such as current, cell voltage, temperature, gas pressure, humidification and gas rate of flow. The experimental setup of the MEA tests will be described in more detail in a future paper. The electrochemical characterisation of the electrodes was performed through current–voltage curves, CV [31] and EIS [32].

During the *V–I* measurements, the fuel cell was operated at 80°C with the hydrogen feed stream humidified by passage through a wash-bottle at a temperature of 80°C. The oxygen was not humidified. We used pure hydrogen and oxygen, both at 2.0 bar. The hydrogen flow was

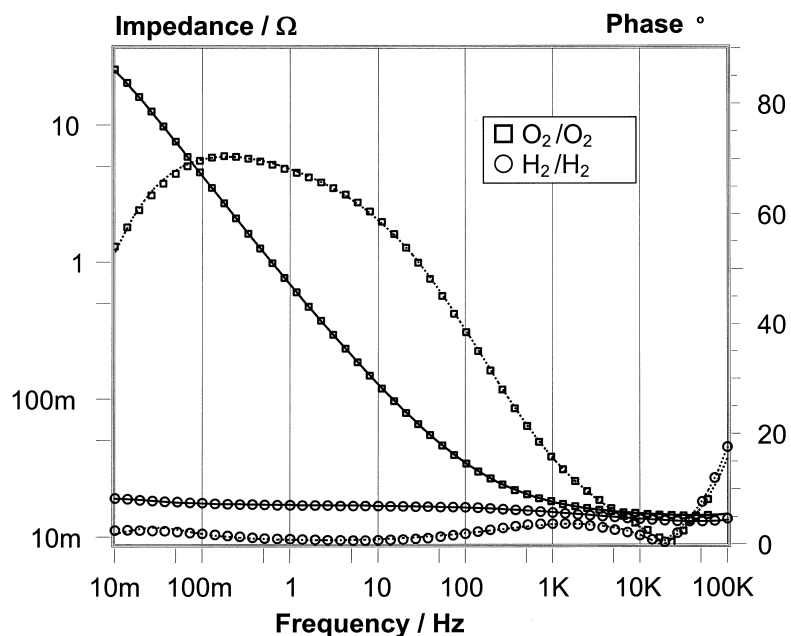Fig. 3. Bode diagram of the EIS, measured at the PEFC (impregnated E-TEK electrodes, Nafion 117), at 80°C, $p_{H_2} = p_{O_2} = 1$ bar, symmetrical gas supply. The solid lines display the impedance magnitudes and the dashed lines the phase shifts of the cathode (□) and the anode (○).
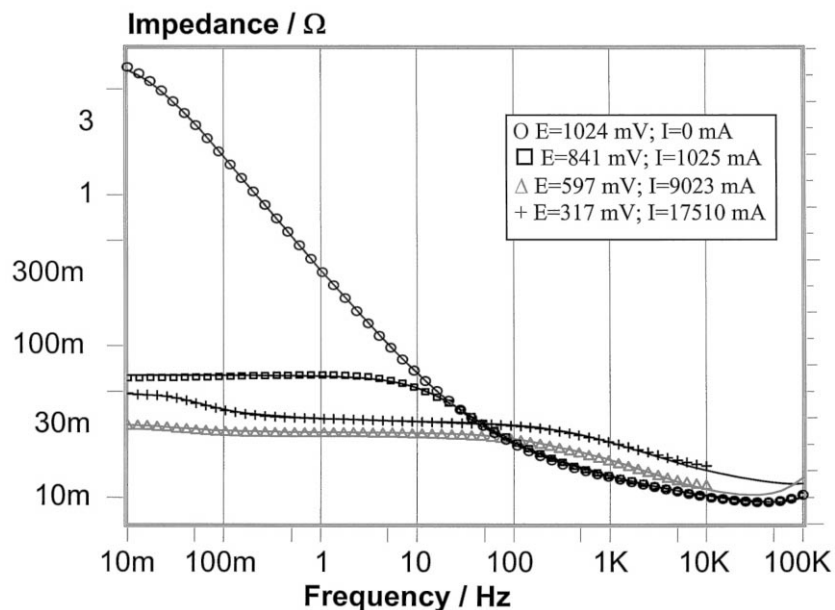
Fig. 4. Bode diagram of the EIS, measured at different cell voltages, PEFC (impregnated E-TEK electrodes, Nafion 117), at 80°C, $p_{H_2} = p_{O_2} = 1$ bar.

''dead end'', wearing sealed channels, whereas the oxygen flow was varied to the cell requirement at different current densities. The oxygen flow at the end of the fuel cell was kept constant. The over-stoichiometric supply of oxygen decreases with higher current densities and was approximately 1.4 at a cell voltage of 500 mV. Fig. 2 shows the V–I characteristics of the electrode produced at one development point for our PEFC electrodes. The V–I characteristics was measured for an MEA with a Nafion 112 membrane (thickness approximately 50 μm) and ultrathin catalytic layers prepared on the membrane. The Pt-loading was 0.07 mg/cm^2 for each electrode.

In order to separate the electrode overvoltages from the cell overvoltage that occurs during load, impedance mea-

surements (EIS) were performed. Measurements at currents up to 25 A have been carried out in combination with an electronic load. Before starting each impedance measurement, the cell was pre-polarised for at least 15 min at the measuring potential to reach steady state conditions. The current densities before and after each impedance measurement have been monitored to prove stability of the cell during measuring times. The DC-current/voltage values have been used to plot steady state current/voltage curves.

A first step was the separation of the anodic impedance, cathodic impedance and the determination of the membrane resistance. Therefore, the fuel cell was operated with a symmetrical gas supply at 80°C with impregnated (Naf-
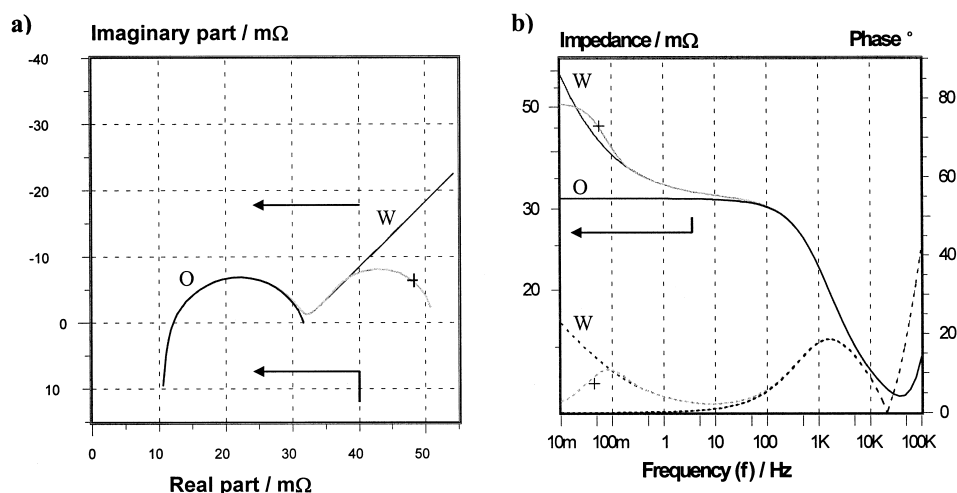

Fig. 5. Nyquist (a) and Bode (b) representation of the spectrum (+) from Fig. 4 and simulated spectra without diffusion (O) and with infinite diffusion (W).

ion suspension) electrodes, at open cell voltage (Fig. 3). Impedance spectra are represented as Bode plots, where the logarithm of the impedance magnitude and phase-shift are plotted vs. the logarithm of the frequency. In the Bode diagram in Fig. 3, in the low frequency range of the spectra, it can be clearly seen that the cell impedance at open cell voltage is determined by the impedance of the cathode. The contribution of the anode can be neglected [15]. The cell impedance at frequencies higher than 10 kHz can be related to the membrane resistance.

The cell impedances (Fig. 4), measured during normal PEFC operation at different cell voltages, show a minimum at approx. 9 A (390 mA cm^{-2}) in the low-frequency range of the spectra. With increasing load of the cell, at lower cell voltages, an increasing cell impedance is observed as, for example, in the spectrum recorded at 17 510 mA. From this increase in cell impedance, we can deduce that, at a higher loading of the cell, an additional overvoltage occurs. From the impedance spectra, it is possible to identify this additional overvoltage as a diffusion overvoltage. In this case, it is a finite diffusion, corresponding to the Nernst-impedance [15–17,33,34].

Given the time constant for mass transport, the impedance related to diffusion is usually found in the lowest sector of the frequency range. Therefore, the impedance has to be measured over a wide frequency range, down to 10 mHz or even lower. To identify and separate the different diffusion processes, it is useful to represent the impedance spectra as Nyquist diagrams (imaginary part vs. real part of the impedance).

In the Nyquist diagram (Fig. 5a), the finite diffusion appears as an additional loop at the lowest part of the frequency range and the infinite diffusion as a straight line with a slope of 1 (real part = imaginary part). In the logarithmic representation of the impedance, the difference of the two kinds of diffusion is not so clear as in the Bode diagram (Fig. 5b).

In order to evaluate the measured impedance spectra, the reaction steps can be translated into an appropriate equivalent circuit that contains various impedance elements representing the reaction steps involved. The main features of the impedance measurements can be explained using the equivalent circuit from Fig. 6 that contains the charge transfer resistance (R_{ct}) and Nernst-impedance (Z_N), parallel to the double layer capacity (C_{dl}) and the high frequency resistance (R_{HF}).
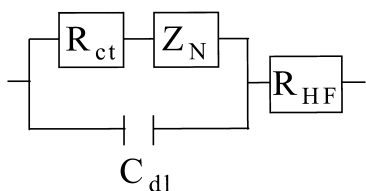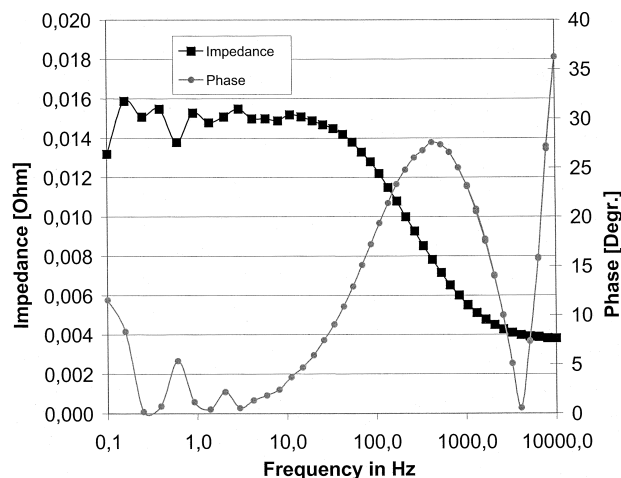

Fig. 7. Bode representation of the impedance spectra measured at 600 mV (840 mA/cm^2), at the PEFC with Nafion 112 membrane; thin electrolyte layer between electrode and electrolyte, Pt-loading 0.07 mg/cm^2, 80°C, $p_{H_2} = p_{O_2} = 2$ bar.

In order to characterise the electrodes prepared by the dry production technique developed at DLR, electrochemical impedance spectra were recorded for PEFCs. The fuel cell and the operating conditions are the same as during the recording of the V–I characteristics (Fig. 2). From the Bode representation of the EIS (Fig. 7) measured potentiostatically at a cell voltage of 600 mV ($I = 840$ mA/cm^2), it is possible to separate the ohmic resistance of the polymer electrolyte membrane from the polarisation resistance of the fuel cell. Comparing the EIS recorded for fuel cells of varying thickness of the membrane, it can be concluded that the ohmic contribution of the thin membranes (Nafion 112) is small, as expected. Additionally, the diffusion impedance due to the water back-diffusion, observed with thick membranes (Nafion 117), is not observed with thin membranes. This can be derived from the different behaviour in the low frequency range in the impedance spectra.

In addition to the influence of the different membranes, the impedance of the electrodes prepared with the DLR technique is lower than was measured for the E-TEK electrodes with a Nafion 117 membrane (Fig. 2). This effect is induced by the lower transport inhibition in the ultrathin electrode film of the DLR electrodes, as expected from simulation studies [35].

4. Physical characterisation

In addition to the study of the electrochemical behaviour of the MEA, physical characterisation is necessary for an understanding of the operation and loss mechanism as well as for optimising the MEA structures. For this

Fig. 6. Equivalent circuit of the PEFC.

purpose, the investigation of single components and complete MEAs is important. The characterisation of new components is not problematic, but after hot pressing the MEA, the components must be separated for analysis. Due to hot pressing, the electrodes and the membrane stick firmly together, so it is not possible to separate the single components from the MEA in a well-defined way. This yields a problem for the characterisation of the components used. For characterisations of MEA structures with SEM [36] and EDX [36], this is relatively unimportant because the local resolution of these methods allows the study of single components for typical cross-sections of MEAs.

With SEM, the structure of the samples can be investigated. The contrast in SEM images for differing materials allows distinction between them. EDX measurements yield information about the elemental distribution and, in combination with SEM, the local elemental distribution can be determined. The SEM is used, for example, to obtain information about layer thickness and uniformity. The samples under investigation were MEAs that had been hot-pressed following electrochemical testing. In order to obtain information about cross-sections, two different procedures were used: (1) by cutting the MEA with a sharp knife, the overall shape of the MEA was preserved, especially that of the carbon cloth, but the electrodes were distorted. In order to avoid distortion of the electrode: (2) the MEA was cooled down to liquid nitrogen temperature (77 K) and snapped. Fig. 8 shows the cross-section of an MEA prepared with the DLR production technique on a 40-μm membrane. The Pt-containing parts of the electrodes (reactive layer) are shown as bright white. It can easily be seen that the thickness of the catalyst layer is
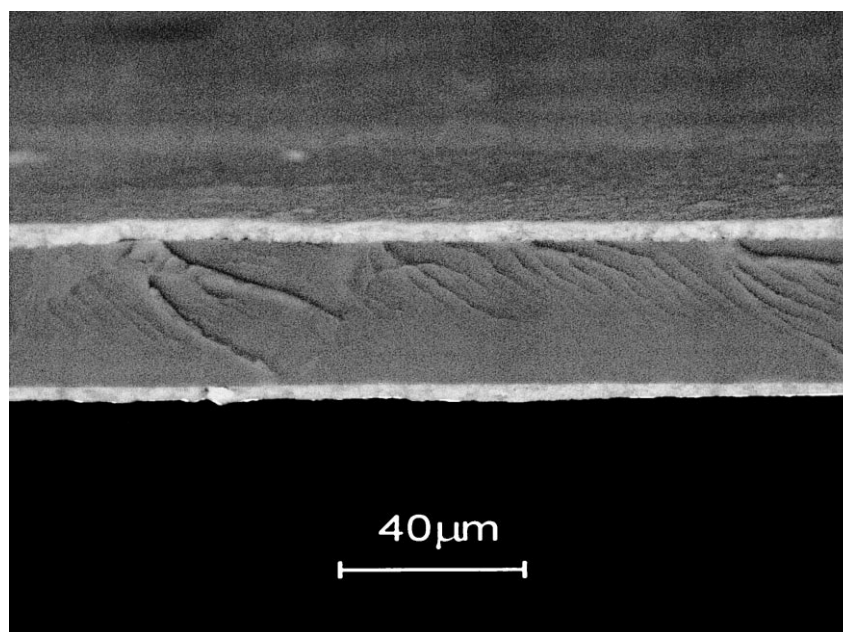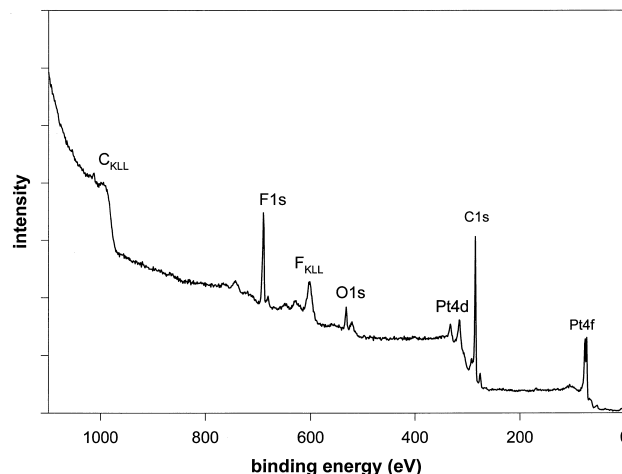

Fig. 9. XPS spectra of an electrode prepared by a dry production technique of the DLR.

fairly constant at 5 μm. The SEM image shows the high degree of uniformity and reproducibility of the electrodes.

As shown with the SEM, the components can be studied individually for a typical cross-section of an MEA. After stripping the backing from the MEA, the structure and elemental distribution in the surface of the reaction layers can be investigated by SEM and EDX.

The chemical composition of the first few atomic layer determines catalytic behaviour. X-ray photoelectron spectroscopy (XPS) allows a determination of the chemical composition of surfaces in these first atomic layers [37]. In addition to element concentrations, XPS yields information about the binding state of the elements. Due to the high surface sensitivity of the method, XPS needs a good

Fig. 8. Cross-section of an MEA with a 40-μm-thick membrane and reactive layers with a thickness of 5 μm.
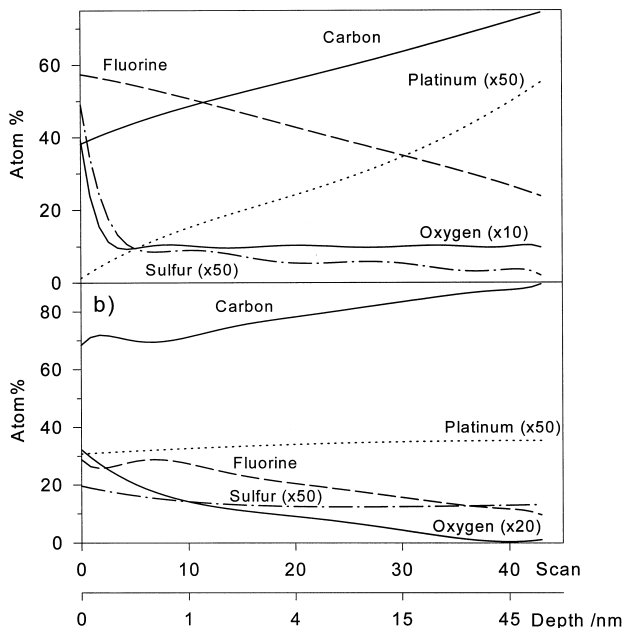
Fig. 10. Depth profile of (a) an E-TEK electrode with Pt/C catalyst as received and (b) an electrode prepared by DLR with Pt/C catalyst.

vacuum and an appropriate sample pre-treatment. As a consequence of this surface sensitivity, the requirement of the separation technique for the MEA to split the electrode and membrane to give a well-defined interface are extremely important: unfortunately, we have not yet found an appropriate method to prepare electrodes from a hot-pressed MEA for XPS measurements. XPS measurements on electrochemically stressed MEA components were performed after electrochemical testing in electrolyte solutions as well

as for cold-pressed MEAs. The pre-treatment of the electrodes for the XPS measurements and the conduit of the XPS measurements is described in Refs. [22,24,25]. Fig. 9 displays the XPS spectrum of an electrode prepared with a dry preparation technique by the DLR. In the spectrum of this electrode, fluorine, carbon, oxygen, sulphur and a small amount of platinum were detected. The fluorine and a part of the carbon are bonded in the PTFE. The other part of the carbon signal is induced by the carbon black that contains the sulphur. In the C1s signal, the portions of carbon in PTFE and carbon black can be distinguished. For this C1s spectrum, PTFE gives a signal at a binding energy of 295 eV, carbon black at a binding energy of 288 eV. The platinum on the carbon black must be covered by PTFE.

The combination of XPS measurements and ion etching allows recording of depth profiles. For this, characteristic ranges of the spectrum were measured for each element of interest. During depth profiling. XPS spectra of F1s in the binding energy range of 700–680 eV, C1s in the binding energy range of 305–280 eV, O1s in the binding energy range of 543–523 eV, Pt4f in the binding energy range of 85–65 eV and S2p in the binding energy range of 185–155 eV were recorded. The element concentrations as functions of the ion etching depth were determined by depth profiling measurements.

The depth profile at the top in Fig. 10 shows the spectrum of the commercial electrode (E-TEK) and the spectrum below the depth profile of an electrode that was produced by our rolling process. In the measurement of the E-TEK electrode, it can be clearly seen, that the platinum concentration increases with the ion etching depth. The
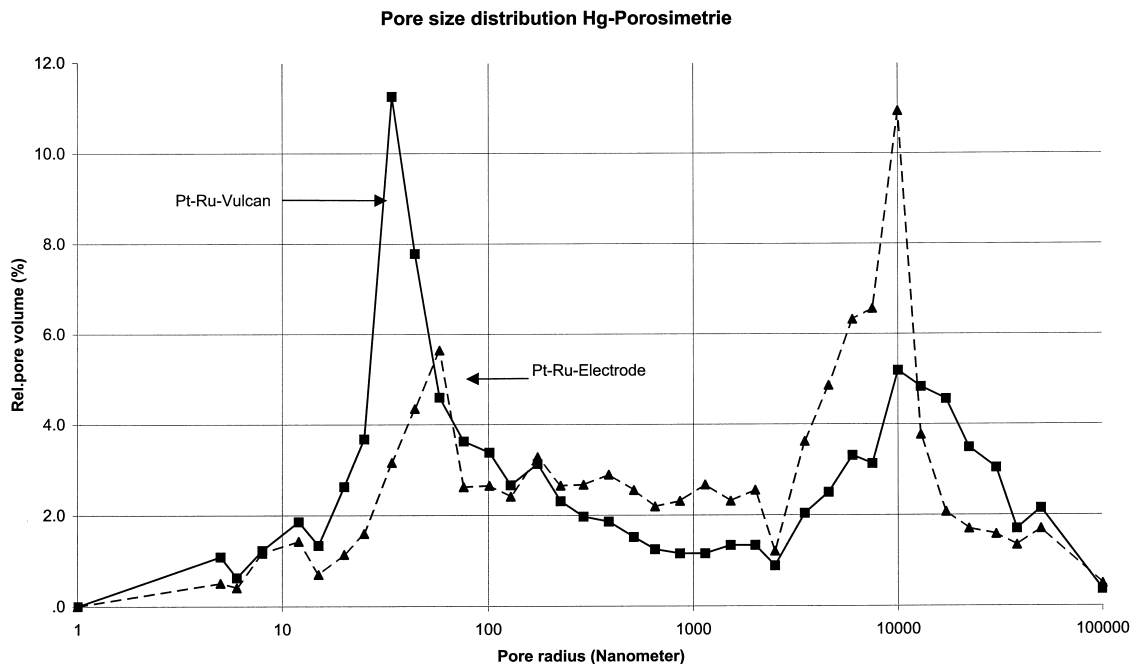

Fig. 11. Pore size distribution of PtRu supported on carbon black (solid line) and an electrode with the catalyst and a single-sided backing (dashed line).

platinum concentration increases from 0.04 up to 1.1 at.% (approx. 15 wt.%) in a depth of 45 nm. The carbon concentration also increases, while, in contrast, the fluorine concentration decreases. This behaviour can be explained by a PTFE film on the surface of the electrode that covers the platinum catalyst and the carbon black. During depth profiling, PTFE and Nafion are decomposed due to the ionising radiation and partially removed from the surface [22,25,38]. Consequently, the signal from the carbon in PTFE decreases and the carbon black signal increases, as demonstrated in Fig. 10. The thickness of the polymer film is approximately 3 nm [19].

For the dry-prepared electrodes, a homogenous elemental distribution was recorded. The reactive layer was prepared from 40 wt.% PTFE and 60 wt.% carbon black with a platinum content of 10 wt.%. The platinum content on the surface of the electrode is approximately 15 wt.%. This means that the platinum is concentrated on the surface of the carbon black. Thus, no polymer film on the rolled electrode could be detected [19,20]. This means the catalytically active platinum on the surface of the dry-prepared electrodes is not covered. Most of the sulphur in the depth profile of the DLR electrode is in the carbon-supported catalyst powder. As a comparison, XPS spectra of the catalyst powders (10, 20 and 40 wt.% Pt) were recorded. These indicate a sulphur concentration of approximately 0.2–0.3 at.%. Thus, the approximately constant sulphur concentration below the electrode surface may be due to sulphur in the carbon catalyst.

Pore features are significant for understanding the transport mechanisms and the structure of the electrodes. Using nitrogen adsorption and mercury porosimetry [39,40], the pore structures of MEAs, single electrodes and of their components were measured. The electrodes consisted of the catalyst supported on carbon black and a carbon backing. Fig. 11 shows the pore size distribution determined by Hg porosimetry measurements for the PtRu supported on carbon black and for a PtRu electrode that was used for DMFCs. Two different pore structures have been found for these electrodes. A pore structure of 10 μm predominates in the carbon cloth backing, whilst a pore structure of 30 nm predominates in the carbon black.

In addition, pore structures of MEAs (MEA) have been measured. Fig. 12 shows the pore size distributions of a hot-pressed MEA for DMFC applications and its components. Of the electrodes examined, one was PtRu supported on carbon black and the other Pt supported on carbon black. The protonic conducting polymer membrane confers no additional porosity. The compressibility of the membrane is compensated for by a measurement of a single membrane, so only the pore structure of the electrode is determined by the porosimetry measurements. A significant difference is observed between the pore size distributions of the two electrodes. The backing of the Pt electrode has a hydrophobic layer on one side and that of the PtRu electrode has hydrophobic layers on both sides. For the single-sided backing, the pore size has a broad distribution between 3 and 30 μm. The measurement of the electrode with the double-sided backing yields a maximum in the pore size distribution at 10 μm. From the porosimetry measurements, it is possible to distinguish the different backings. The pore size distribution of the MEA is a superposition of the pore size distributions of the single electrodes, but the pore system of the backings is
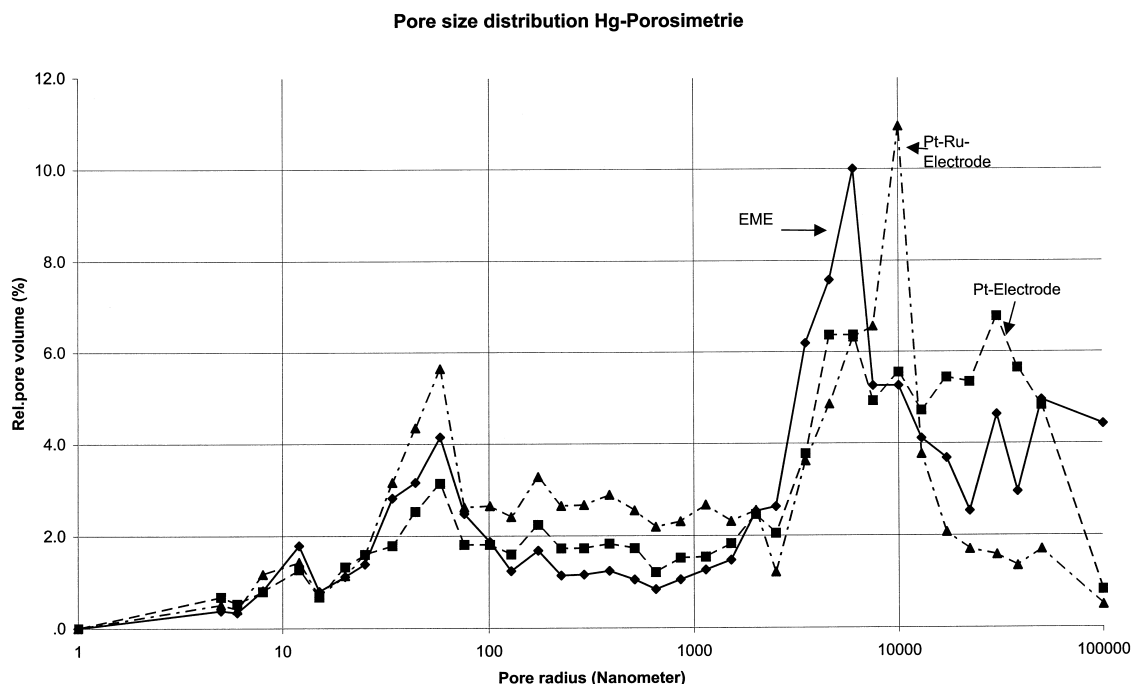

Fig. 12. Pore size distribution of an MEA (solid line) and its PtRu electrode (dash–dotted line) and Pt electrode (dashed line) before hot pressing.

shifted to lower pore radii. This is most likely induced by hot pressing. A similar effect was observed by BET measurements of the pore size distribution of the carbon black after pressing by a rolling process in a calender [19]. The surface determined by the porosimetry measurements was reduced somewhat, but not significantly, after hot pressing as well as impregnation with Nafion suspension. The porosimetry allows measurement of the pore size distribution of electrodes in an MEA structure as well as that of single electrodes. This is important for the characterisation of electrochemically stressed MEAs in studying their degradation processes. In contrast to the DMFC electrodes, for porosimetry measurements on PEFC electrodes with ultrathin reaction layers, the absolute contribution of the pore structure of the reactive layer is insignificant compared to the total pore structure. However, for these electrodes, only the pores in the backing material are important for the transport of gases and water. So, in both cases (thick and thin reactive layers), the relevant pore structures can be satisfactorily studied by porosimetry measurements.

5. Degradation

The electrochemical behaviour of electrode assemblies changes during the lifetime. Changes are especially observed in the dependence of the $V-I$ characteristics during humidification. This indicates that water transport and balance differs for new and electrochemically stressed electrodes. It seems that the pores can be flooded more easily by water in stressed electrodes than in newly prepared electrodes. The water balance in the electrodes is significantly determined by the membrane and the mixture of the hydrophobic and hydrophilic parts of the backing. Hydrophobicity is induced by PTFE that is present in the backing and the electrode.

XPS investigations of the polymers in gas diffusion electrodes have demonstrated that the PTFE and Nafion can be partially decomposed or changed by electrochemical stressing [18,21,22,25,38]. The C1s spectra of three electrodes are shown in Fig. 13. The measurements were performed on commercial electrodes that have a polymer-covered surface. Two of the electrodes were electrochemically stressed under a fuel cell operating conditions. The MEA was not hot-pressed, so contact between membranes and electrodes was weak and the electrodes could be separated from the MEA after operating in the fuel cell. Due to the absence of a reproducible separation process for electrodes of well-prepared, hot-pressed MEAs, XPS measurements on electrochemically stressed electrodes cannot be performed. Two different binding states of carbon can clearly be distinguished. The first, at the higher binding energy, is related to the PTFE and the other is related to the carbon in the carbon black. The lower spectrum is the spectrum of an unused electrode. The carbon is mainly bonded to the PTFE. The XPS spectra of the electrode,
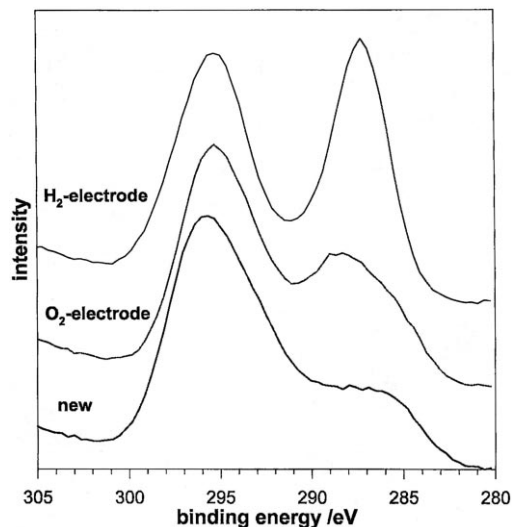

Fig. 13. C1s spectra of E-TEK electrodes as received, used as cathode and used as anode (from bottom to top).

which was used as an oxygen electrode, is nearly unchanged as compared to that of a new electrode. The carbon in the graphite state has increased slightly in this electrode. For the electrode that was used as an anode, this state has increased significantly. This indicates that a change occurs in the PTFE, an effect that is stronger in the anode. Similarly, decomposition of the PTFE during electrochemical operation was observed for rolled electrodes for alkaline fuel cells in previous XPS studies [22] and for the PEFC electrodes that were used in H_2SO_4 [18]. Similarly, the decomposition of the PTFE in gas diffusion electrodes based on polymer electrolyte membranes can be changed according to the electrochemical loading [25,38]. A change in the PTFE in the electrode or the backing, induced by electrochemical processes, can explain the change in the influence of humidification. This hypothesis should be checked with further measurements.

In the XPS study of the spent electrodes, depth profiles were measured. At the beginning of depth profiling, a lower oxygen concentration in the hydrogen electrode than in the new and oxygen electrode was measured. The depth profiles of the electrode operating as cathode and that of the new electrode are very similar. Fig. 14 shows the XPS spectra of platinum for both spent electrodes recorded during the depth profile measurements. For the cathode, as well as for the new electrodes, the platinum catalyst is covered by a polymer film at the start of the depth profile measurement and the platinum concentration increases with the ion etching time. In contrast, the electrode that was used as a hydrogen electrode shows a dramatical change in the platinum concentration on the surface. The platinum concentration on the anode is significantly reduced. The Pt4f spectra of the anodes was increased by a factor of 25 as compared to the spectra of the cathode. At the beginning of depth profiling, the platinum concentration in the
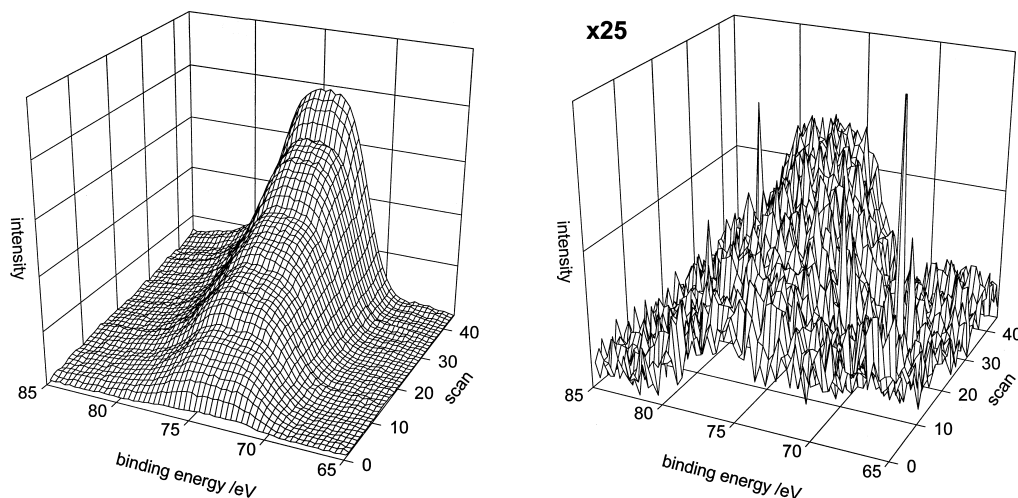
Fig. 14. (a) Pt4f spectra of an E-TEK electrode used as cathode in a PEFC during depth profiling. (b) Pt4f spectra of an E-TEK electrode used as anode in a PEFC during depth profiling.

hydrogen electrode is close to the detection limitation of the XPS instrument and increases during the depth profiling by a factor 2–5. The decrease of the platinum concentration can be explained by a change in the platinum distribution. It is well known that platinum–hydrogen complexes have a high mobility [41]. If the platinum clusters move together and build up larger three-dimensional clusters, less platinum remains on the surface and more platinum lies at depth and cannot be detected in XPS spectra. Another possible explanation is that the platinum has migrated to the interface between the membrane and the electrode and has adhered to the membrane upon separating the electrode from the MEA. The membrane was not investigated by XPS, so it cannot be decided which platinum diffusion mechanism removes platinum from the electrode surface investigated. In a CV experiment in a half cell with sulphuric acid and the same electrode, the platinum concentration on the electrode surface does not change so markedly [18]. From this, it can be assumed that the diffusion to the membrane–electrode interface is the important mechanism.

From the XPS measurements on spent electrodes, it can be deduced that platinum migrates in the hydrogen electrode, but not in the oxygen electrode. The polymer in the electrodes is decomposed during electrochemical treatment. This decomposition process seems faster on the anode than on the cathode. The degradations observed may induce a change in the electrochemical behaviour.

6. Conclusions

The new dry production technique developed by DLR for ultrathin electrodes has several advantages. The new production technique allows a simple production of MEAs and electrodes, and has a high degree of automation.

Furthermore, this technique and the production units can be scaled up for industrial requirements. During all production steps, no solvents are required. Therefore, the process is environmentally benign and in addition, loss of time caused by drying steps is avoided. Due to the preparation of ultrathin reactive layers for MEAs for PEFC applications, very low noble metal loadings are possible. All the advantages described yield a low cost production technique, with a high capability for commercial use.

An additional advantage is that the process is very flexible and can be adapted to other requirements as in DMFC electrodes with gradated layer structures or other materials.

The electrochemical and the physical characterisation of these electrodes and MEAs has been used for the determination of materials' loss processes and their causes that occur during MEA operation under different conditions. Furthermore, from the electrochemical and physical investigations, information has been obtained about the principal reaction mechanism and structure of the MEA. With this information, and knowledge from the characterisation and basic investigation, the preparation technique has been improved. Presently, it is possible to produce electrodes and MEAs with excellent electrochemical performance, comparable with commercially available MEAs. The quality control of the production technique results directly from these investigations.

References

[1] Daimler-Benz HighTech Report, 1997, p. 20.

[2] D. Bevers, N. Wagner, M. von Bradke, Int. J. Hydrogen Energy 23 (1997) 57.

[3] D. Bevers, N. Wagner, Patent DE 19509749 C2, 1997.

[4] M. Wilson, S. Gottesfeld, J. Appl. Electrochem. Soc. 22 (1992) .

[5] S. Gottesfeld, T.A. Zawodzinski, Polymer electrolyte fuel cells, in: R.C. Alkire, H. Gerischer, D.M. Kolb, Ch.W. Tobias (Eds.), Advances in Electrochemical Science and Engineering, Vol. 5, Wiley-VCH, Weinheim, 1997, p. 229.

[6] M. Uchida, Y. Aoyama, E. Eda, A. Ohta, J. Electrochem. Soc. 142 (1995) 4143.

[7] M. Uchida, Y. Fukoua, S. Sugawara, E. Eda, J. Electrochem. Soc. 143 (1996) 2245.

[8] M. Wöhr, K. Bolwin, W. Schnurnberger, M. Fischer, W. Neubrand, G. Eigenberger, Int. J. Hydrogen Energy 23 (1997) 213.

[9] J.R. Macdonald, D.R. Franceschetti, J. Electroanal. Chem. 307 (1991) 1.

[10] D.B. Zhou, H. Vander Poorten, Electrochim. Acta 40 (1995) 1819.

[11] T.E. Springer, T.A. Zawodzinski, M.S. Wilson, S. Gottesfeld, J. Electrochem. Soc. 143 (1996) 587.

[12] A. Parthasarathy, B. Dave, S. Srinivasan, A.J. Appleby, C.R.S. Martin, J. Electrochem. Soc. 139 (1992) 1634.

[13] A. Parthasarathy, S. Srinivasan, A.J. Appleby, J. Electrochem. Soc. 139 (1992) 2530.

[14] V.A. Paganin, C.L.F. Oliveira, E.A. Ticianelli, T.E. Springer, E.R. Gonzalez, Electrochim. Acta 43 (1998) 3761.

[15] N. Wagner, W. Schnurnberger, B. Müller, M. Lang, Electrochim. Acta 43 (1998) 3785.

[16] B. Müller, N. Wagner, D. Bevers, Characterization of electrode membrane assemblies in polymer electrolyte fuel cells operating with H_2 or H_2 /100 ppm CO mixtures using AC impedance spectroscopy, to be published in J. Power Sources.

[17] M. Lang, R. Henne, G. Schiller, N. Wagner, Production and Characterization of Vacuum Plasma Sprayed Anodes for Solid Oxide Fuel Cell, Proc. of the 5th Int. Symp. on SOFC, Proc. Vol. 97-40, The Electrochem. Soc., 1997, p. 461.

[18] J.M. Rheaume, B. Müller, M. Schulze, J. Power Sources 76 (1998) 60.

[19] M. Schulze, N. Wagner, G. Steinhilber, E. Gülzow, M. Wöhr, K. Bolwin, Proc. Fuel Cell Seminar, Orlando, 1996, p. 663.

[20] E. Gülzow, A. Helmbold, N. Wagner, R. Reissner, W. Schnurnberger, M. Schulze, Characterization and Innovative Production Technique for PEFC and DMFC Electrodes, 12th World Hydrogen Conference, Argentina 1998, Proceedings, p. 1653.

[21] E. Gülzow, A. Helmbold, R. Reißner, M. Schulze, N. Wagner, M. Lorenz, B. Müller, T. Kaz, Proceeding Fuel Cell Seminar 1998, Palm Springs, USA, 16–19 November, p. 469.

[22] M. Schulze, K. Bolwin, E. Gülzow, W. Schnurnberger, Fresenius' J. Anal. Chem. 335 (1995) 778.

[23] E. Gülzow, B. Holzwarth, W. Schnurnberger, M. Schulze, G. Steinhilber, N. Wagner, Hydrogen Energy Progress IX, Proc. World Hydrogen Energy Conference, Paris, 1992, p. 1507.

[24] M. Schulze, M.V. Bradke, R. Reissner, M. Lorenz, E. Gülzow, Characterization of polymers in PEFC electrodes with EDX and XPS, Fresenius' J. Anal. Chem., in press.

[25] M. Schulze, M. Lorenz, N. Wagner, E. Gülzow, XPS analyzing of the degradation of Nafion, Fresenius' J. Anal. Chem., in press.

[26a] A. Helmbold, Verfahren zur Herstellung von Funktionsschichten für Brennstoffzellen Deutsches Patent DE 197 57 492 A 1, 1999.

[26b] D. Bevers, N. Wagner, Verfahren zur Herstellung eines Verbundes aus Elektrodenmaterial, Katalysatormaterial und einer Festelektrolytmembran, Patentschrift, DE 195 09 749 C2.

[27] D. Bevers, N. Wagner, M.V. Bradke, Innovative production procedure for low cost PEFC electrodes and electrode membrane structures, 11th World Hydrogen Conference, Stuttgart, Germany 1996, Proceedings, p. 1767.

[28] D. Bevers, E. Gülzow, A. Helmbold, B. Müller, Innovative production procedure for PEFC electrodes, Fuel Cell Seminar, Orlando, FL, 1996, Proceedings, p. 668.

[29] D. Bevers, N. Wagner, M.V. Bradke, J. Hydrogen Power 63 (1996) 193.

[30] E. Gülzow, J. Power Sources 61 (1996) 98.

[31] D.K. Gosser, Jr., Cyclic Voltammetry, Simulation and Analysis of Reaction Mechanisms, VCH Publisher, Weinheim, 1994.

[32] J.R. Macdonald (Ed.), Impedance Spectroscopy, Wiley, New York, 1987.

[33] C. Gabrielli, Use and Applications of Electrochemical Impedance Techniques, Technical Report 24, Solar Instruments, 1990.

[34] H. Göhr, IM6-Impedanzmeßsystem, 1997.

[35] D. Bevers, M. Wöhr, K. Yasuda, K. Oguro, J. Appl. Electrochem. 23 (1998) 12.

[36] M. Henzler, W. Göpel, Oberflächenphysik des Festkörpers, Teubner Studienbücher, Stuttgart, 1991, pp. 107, 282.

[37] G. Ertl, J. Küppers, Low Energy Electron and Surface Spectroscopy, VCH-Verlagsgesellschaft, Weinheim, 1985, p. 70.

[38] M. Schulze, E. Gülzow, R. Reißner, N. Wagner, M. Lorenz, W. Schnurnberger, X-Ray Photoelectron Spectroscopy Investigations on Nafion Membrane, Joint International Meeting ECS/ISE, Paris, France, 1997.

[39] Carlo Erba Microstructure Line No. 5, 1987, p. 1.

[40] Carlo Erba Microstructure Line No. 19, 1987, p. 2.

[41] M.S. Wilson, F.H. Garzon, K.E. Sickafus, S. Gottesfeld, J. Electrochem. Soc. 140 (1993) 2872.